

Semantics Disentanglement and Composition for Versatile Codec toward both Human-eye Perception and Machine Vision Task

Jinming Liu^{1,2}, Yuntao Wei², Junyan Lin²,
Shengyang Zhao², Heming Sun⁴, Zhibo Chen³, Wenjun Zeng², Xin Jin^{2†}

¹Shanghai Jiao Tong University

²Ningbo Institute of Digital Twin, Eastern Institute of Technology, Ningbo, China

³University of Science and Technology of China

⁴Yokohama National University

Abstract

While learned image compression methods have achieved impressive results in either human visual perception or machine vision tasks, they are often specialized only for one domain. This drawback limits their versatility and generalizability across scenarios and also requires retraining to adapt to new applications—a process that adds significant complexity and cost in real-world scenarios. In this study, we introduce an innovative semantics **DIS**entanglement and **CO**mposition **VER**satile codec (**DISCOVER**) to simultaneously enhance human-eye perception and machine vision tasks. The approach derives a set of labels per task through multimodal large models, which grounding models are then applied for precise localization, enabling a comprehensive understanding and disentanglement of image components at the encoder side. At the decoding stage, a comprehensive reconstruction of the image is achieved by leveraging these encoded components alongside priors from generative models, thereby optimizing performance for both human visual perception and machine-based analytical tasks. Extensive experimental evaluations substantiate the robustness and effectiveness of **DISCOVER**, demonstrating superior performance in fulfilling the dual objectives of human and machine vision requirements.

1. Introduction

Image compression has become an essential aspect of data management, especially as the demand for image transmission and storage continues to grow. Traditionally, image compression techniques like JPEG [1], HEVC [2], and VVC [3] have focused on optimizing visual fidelity. With the rapid development of deep learning, advanced learned-based methods [4–6] have demonstrated superior performance over traditional techniques on standard fidelity metrics such as PSNR and MS-SSIM. For instance, Liu *et al.* [4] utilize mixed transformer-CNN architectures to capture both global and local information of the image to improve learned-based image compression (LIC). Li

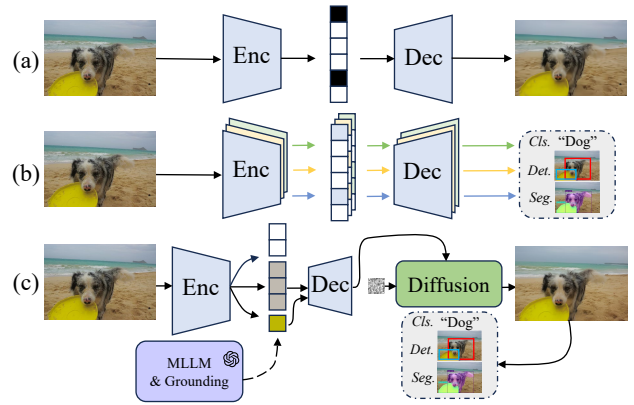


Figure 1. The codec paradigm of (a) human perception (b) machine vision (c) proposed **DISCOVER**. It leverages the task-level MLLMs and image-level grounding modules for semantic analysis and disentanglement, transmitting only the bit-streams of task-related elements. At the decoding stage, it incorporates priors from generative models to supplement information, producing high-quality images that simultaneously meet the requirements of human perception and machine vision tasks.

et al. [5] propose the Frequency-Aware Transformer (FAT) block to perform multiscale directional analysis for LIC. Both methods achieve performance that significantly surpasses that of the latest standardized codec VVC. Moreover, some approaches [7–10] integrate generative models to compress images to extremely low bitrates while preserving quality suited for human visual perception. For example, Careil *et al.* [10] proposed decoding with iterative diffusion models instead of traditional feed-forward decoders [11, 12], resulting in significantly improved visual quality. However, these methods are all limited to be optimized for human perceptual fidelity, which seriously constrains their utility in wider machine vision tasks, like object detection, segmentation, classification, etc [13–15].

The above-mentioned machine tasks influence numerous practical applications, such as intelligent traffic systems, autonomous driving, and chat-bot [16, 17]. Hence, efficient image compression for machines is crucial in re-

ducing bandwidth and storage requirements w.r.t real applications. In response, the task of image coding for machine (ICM) [18–22] has emerged, focusing on the joint optimization of compression rates and downstream tasks accuracy. For instance, Chamain *et al.* [23] proposed a joint optimization of codecs and downstream task networks to enhance specific machine vision tasks. Chen *et al.* [22] utilize a prompt tuning method to transfer base codec to another machine vision task. Li *et al.* [21] use spatial-frequency adapters to efficiently tuning codec for other tasks. However, these works go to the other extreme - making the codec more suitable for supporting machine tasks, while ignoring the basic need to ensure the perceptual quality of the reconstructed image for human watching. Besides, another drawback as shown in Fig. 1(b), most of these ICM approaches typically require retraining the codec many times (or training many different codecs) to adapt to different scenes or tasks, which imposes significant overheads and computational costs for practical deployment.

In this paper, we propose a new compression paradigm of semantics **DIS**entanglement and **CO**mposition **VER**satile coding (DISCOVER), which could simultaneously satisfy both human visual perception and machine vision tasks, as shown in Fig. 1. First, semantics analysis and disentanglement are performed at the encoder side, wherein we use multimodal large language models (MLLMs, e.g., ChatGPT 4o [24]) to do task reasoning, generating some potential task-related prior information as a guide for subsequent compression. Note that, this process runs only once to avoid encoding burden even for multi-image compression. Based on such prior, that denoted as candidate semantic labels shown in Fig. 2, we then take a visual grounding module [25] as a filter for filtering image-irrelevant labels and parsing the input image to be compressed, to obtain more detailed semantic information like object class and localization (bounding box). This operation actually disentangles the whole image into multiple key semantic elements (i.e., different objects) and the rest background content. Afterward, we accordingly encode the disentangled objects and background separately to get a final well-structured bitstream. In this way, only transmitting partial specific bitstreams, our codec can support the specific downstream machine tasks, which significantly saves bandwidth costs. At the decoder side, our approach uses a kind of generative model [26–29] to reconstruct the complete image based on the partially transmitted bitstream. Such AI-generated content (AIGC) by generative model supplements the non-transmitted information of the original input image, allowing our DISCOVER to meet the requirements of human watching as well. The contributions of this paper are summarized as follows:

- We propose a new compression paradigm based on semantics disentanglement and composition, enabling

structured coding and reassembly tailored to various tasks, which accommodates both machine vision and human perception requirements.

- We are the first to together leverage the task-level MLLMs and image-level grounding module before encoding, to extract essential guidance for semantic disentanglement, which makes the codec encoder become task-aware and the bitstream semantically structured. This property allows partial transmission so as to largely save bandwidth.
- We also develop a generative diffusion-based decoding and reconstruction method, which gets the decompressed image results by composing the disentangled elements while leveraging prior knowledge from generative models to supplement non-transmitted components.

Experimental results demonstrate that our method achieves superior performance in both machine vision and human perception tasks. Specifically, setting VTM-12.1 as the anchor, we can achieve BD-rates [30] of -80.41%, -80.32%, and -77.63% on object, segmentation, and classification tasks, respectively. Meanwhile, in the detection task, transmitting only the task-related bitstream achieves a BD-FID [31] of -45.615, indicating that the reconstructed images align well with human perception.

2. Related Works

2.1. Image Compression

Image compression aims to encode original images into a format that is both compact and retains high fidelity. Traditional image codec [1–3, 32, 33] has witnessed several decades of developments, generally consisting of handcraft sub-modules like intra-prediction, discrete cosine/wavelet transformation, quantization, and entropy coding. In recent years, learned-based codecs [4–6, 11, 34–36] began to utilize neural networks to optimize distortion and bitrate. These data-driven methods have demonstrated superior rate-distortion performance compared to traditional approaches. With the advancement of AI-generated content (AIGC) technologies [26, 27, 37], some methods have shifted focus from image fidelity to satisfying human perception, achieving satisfactory reconstructed image quality at extremely low bitrates. On the other hand, as machine vision is increasingly used in practice, image coding for machine (ICM) [38–43] is developing to satisfy machine vision tasks like image classification, detection, segmentation, etc. However, many machine task-oriented methods are typically designed for specific scenarios and often require retraining when transferred to different settings. In contrast, in this work, our proposed versatile codec DISCOVER can adapt to a variety of scenarios, covering both human and machine requirements, without any retraining.

2.2. Multi-modal Large Language Model and Visual Image Grounding

Multimodal Large Language Models (MLLMs) [24, 44–46] have experienced rapid advancements over the past few years, showcasing remarkable capabilities in cross-modal understanding and generation. They [24, 45, 47–49] leverage massive high-quality multimodal datasets and extensive model parameters to deliver unparalleled performance. The sensitivity to fine details and the robustness in handling complex tasks make MLLMs widespread. One of the key challenges faced by multimodal models is the complex natural image data, which contains a significantly greater number of tokens and presents more intricate details than text [50, 51]. When processing images, models are often required to actively or passively distill key information from the visual data. This distillation process enables the model to discern which elements are crucial for specific tasks, distinguishing effectively between the most critical and less significant elements. Based on these findings, this paper introduces ChatGPT-4o [24] to achieve semantic disentanglement, which enables the compression model to automatically identify and differentiate between the most critical and less significant elements for each task.

Visual grounding is also close to our work, in which the task aims to locate the most relevant objects or regions in an image based on a natural language query [52–54]. The recent popular open-set Grounding DINO [25] has made grounding approaches more applicable to real-world scenarios, which utilizes cross-modal alignment and contrastive learning methods to filter out the most relevant text during the inference process and achieve precise localization. In this paper, we leverage the open-set capabilities of Grounding DINO by feeding it a large number of candidate semantic labels voted by MLLMs, which ultimately filter the labels and generate corresponding localization information, achieving an effective semantics analysis and disentanglement for the subsequent compression.

2.3. Image Generation

Recently, diffusion models [55–58] have demonstrated remarkable capabilities in image generation by learning to approximate data distributions through the iterative denoising of a noised input. Consequently, they can generate high-quality, complete images from inputs with limited information, such as text, semantic maps, or depth maps [26]. Some studies [7, 10] have attempted to apply this capability to image compression, transmitting only text and downsampled images/features to the decoder, which then employs diffusion to generate visuals that satisfy human vision. However, these approaches do not fully exploit diffusion’s potential for semantic composition and generation. In our work, we further explore the potential of diffusion models for image compression, by performing different semantic composi-

tions based on the partially transmitted bitstream using diffusion, to generate the corresponding complete image so as to meet the needs of different scenes or tasks.

3. Methodology

Overview. Different from the previous image compression methods focused exclusively on either human perception [8, 10, 59] or machine vision [18, 22, 60], our framework of DISCOVER, as illustrated in Fig. 2, is a versatile codec for both human watching and machine tasks that can adapt to various scenarios without retraining/redesigning. Firstly, it utilizes MLLM and grounding modules to analyze and disentangle the semantics of the input image. This enables subsequent semantic-structured encoding, where only task-related information is encoded and transmitted for the machine tasks, significantly reducing bit overheads. Finally, the decoded image can be completely generated by composing the transmitted information with the generative diffusion prior, meeting the requirements of human watching.

3.1. Semantics Analysis by MLLM and Grounding

Previous research [8, 19, 36, 61] has demonstrated that analyzing images from a semantic perspective can better meet the requirements of human perception or machine vision at the same bit rate, compared with fidelity-based methods [4, 5, 11, 12]. However, these methods extract semantics solely for a single task, lacking the ability to adaptively extract diverse semantics for different scenarios, which limits their transferability across varied tasks. In this work, we first employ MLLM for a global understanding of the task (requiring only a single inference per task, making the overhead negligible). Then, a grounding model [25] is used to perform a one-step analysis of each image, extracting detailed semantic information like object class and localization (denoted as a bounding box).

3.1.1 Task Understanding by MLLM

Multimodal large models offer exceptional versatility for a wide range of tasks. By capitalizing on this capability, as Fig. 2 shows, we guide ChatGPT-4o [24] to develop a global understanding of the task to generate some candidate task-related semantic labels for the current task, which provides potential task-related prior information as a bias for the subsequent process, and aligns closely with task requirements.

Specifically, we design a prompting method, as shown in Algorithm 1, which aims at guiding the model through a structured understanding of each task. The prompt firstly directs the assistant to assess the “granularity required by the task”, which allows the assistant to generate labels at an appropriate level of granularity based on specific task requirements. After that, it requests over 100 category-specific labels, promoting both coverage and relevance. This design supports appropriate identification and categorization of key information, thereby promising both task performance and

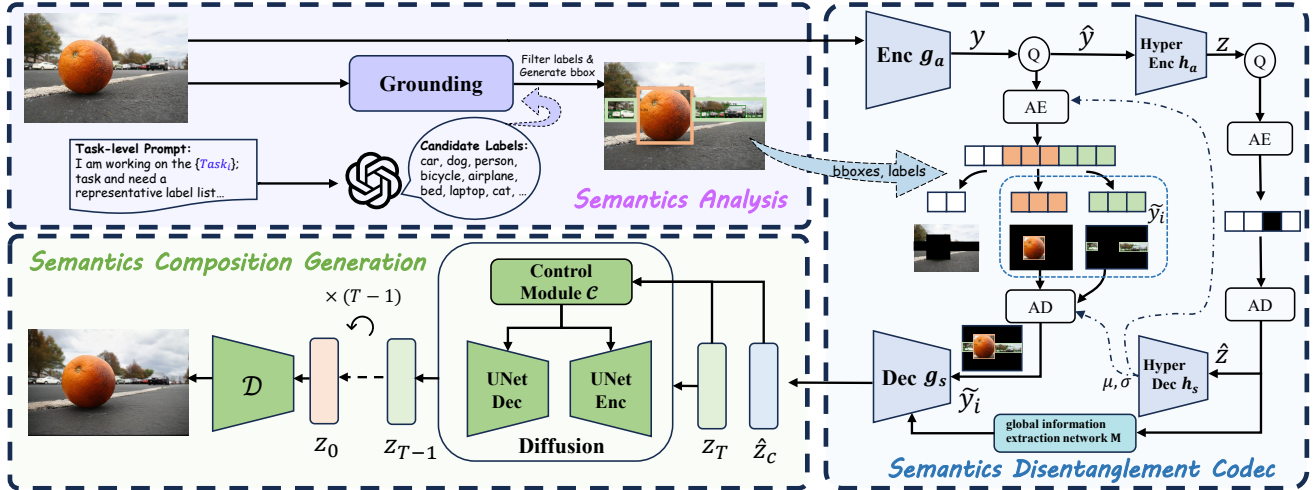


Figure 2. The framework of DISCOVER: (1) First, we use MLLM and grounding model to perform *semantic analysis* and extract the location information of task-related objects. (2) The information is then used for *semantic disentanglement* encoding, transmitting only task-related information. (3) Finally, we leverage the transmitted information and diffusion priors for *semantic composition generation*.

Algorithm 1 Prompt for labels generation

1. Suppose you are an AI assistant and now need to generate task-related object labels based on the task.
2. The number of labels should not be fewer than 100, and the labels should cover a wide range of categories while maintaining appropriate granularity.
3. First, you should determine the granularity required by the task, and then generate the corresponding labels.
4. For example:
 - For some tasks, something that can't be detected, such as the sky or rivers, shouldn't be included as labels.
 - For some tasks, it is necessary to include more comprehensive information about the image, and it needs overly general categories.
5. I am working on the $\{Task\}$ and need a representative label list.
6. The task description is as $\{Task\ Description\}$.

model effectiveness. Also, this prompt framework also enables flexible task adaptation by adjusting $\{Task\}$ and $\{Task\ Description\}$ —where $\{Task\ Description\}$ can be generated by ChatGPT-4o or manually defined—so we can easily switch between different tasks without reconfiguration.

Discussion. In fact, in our initial attempts, we generated labels individually for each image by performing a separate MLLM analysis per image. However, this approach introduced two main issues: (1) repeated calls to ChatGPT-4o results in substantial additional computational and communication costs, and (2) deploying local open-source multimodal models for each image not only incurs high computational overhead but also frequently leads to hallucinations or misunderstandings due to limited model performance, ul-

timately compromising the final output quality. In our current design, we address these challenges by conducting a single global analysis of the task using ChatGPT-4o. This approach incurs negligible overheads while delivering superior performance compared to per-image inference with local open-source multimodal models. Additional details and generated task-specific label lists are provided in the supplementary materials.

3.1.2 Visual Grounding with Task-related Labels

After the MLLM provides task-level priors, we use a visual grounding model to obtain more detailed image-level semantic information like the object category and localization (bounding box). Specifically, Grounding DINO [25] is utilized to filter out image-irrelevant semantic labels and retain only those most relevant to the image. Furthermore, it provides the corresponding localization of these labels within the image. As shown in Fig. 3, we input the generated semantic labels (often more numerous than the labels in the images) alongside the images into Grounding DINO. First, multi-scale image and text features are extracted using separate backbones, such as BERT [62] for text and Swin Transformer [63] for images. These vanilla features are then processed in a feature enhancer for cross-modal fusion, integrating the information across modalities effectively.

After extracting cross-modal text features f_{text} and image features f_{img} , a filter module is applied that filters out superfluous and irrelevant image features under the supervision of f_{text} . The selected image features are used as the cross-modality queries q , which, along with image features f_{img} and text features f_{text} , are then input into the cross-modality decoder. Finally, the decoder outputs predicted object bounding boxes and extracts corresponding

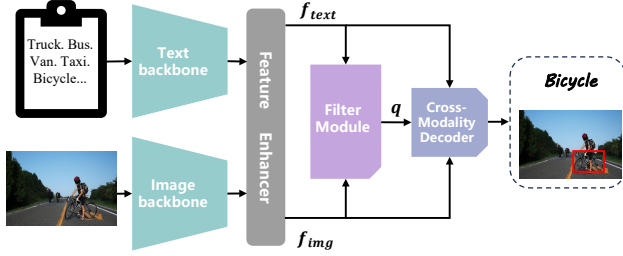


Figure 3. The labels and localization generation process of grounding modules for the vehicle classification task. Different from the general detection, this design could filter out task-related objects (“bicycle”) for the subsequent compression.

labels utilized as prior information to aid subsequent compression encoding.

3.2. Semantics Disentanglement Codec

After acquiring the task-related objects and regions in the image, we based on this prior information to perform semantics disentanglement encoding, which divides the extracted objects and the background into separate groups for compression, as shown in Fig. 2. In this way, only transmitting partial specific bitstreams, our codec can support the specific downstream machine tasks, which significantly saves bandwidth costs.

Following prior image compression works [4, 12], the base codec of DISCOVER comprises three components: an encoder, a hyper-prior path, and a decoder. Firstly, the encoder g_a extracts a compact latent code $\hat{\mathbf{y}}$ from the input image \mathbf{x} . Furthermore, using the location information \mathbf{l}_i for task i derived from the grounding model [25], $\hat{\mathbf{y}}$ is disentangled into different elements. When facing specific tasks, only the task-related component $\tilde{\mathbf{y}}_i$ is transmitted to the decoder. On the other hand, the complete $\hat{\mathbf{y}}$ is downsampled by the hyper encoder h_a to create side information \mathbf{z} , which is quantized as $\hat{\mathbf{z}}$ and then transmitted to the decoder to help approximate the distribution of $\hat{\mathbf{y}}$ for arithmetic coding. The entire encoding process can be defined as:

$$\tilde{\mathbf{y}}_i = g_a(\mathbf{x}|\mathbf{l}_i) \quad \hat{\mathbf{z}} = h_a(g_a(\mathbf{x})) \quad (1)$$

On the decoder side, the coarse global information is extracted also from $\hat{\mathbf{z}}$ using a global information extraction network M composed of two transposed convolutional layers and one convolutional layer, and is then input into the decoder g_s alongside the task-related component $\tilde{\mathbf{y}}_i$. It is crucial to note that our decoder’s reconstruction target diverges from traditional image compression that attempts to reconstruct the original image; instead, our approach aims to reconstruct the diffusion latent code z_c that is obtained after inputting the original image into the diffusion VAE encoder \mathcal{E} , thereby facilitating better integration with the diffusion model during subsequent generative composition. Ultimately, through our proposed DISCOVER codec, we

reconstruct the latent code \hat{z}_c that encapsulates the transmitted task-related information and coarse global information. The entire decoding process can be defined as:

$$\hat{z}_c = g_s(\tilde{\mathbf{y}}_i, M(\hat{\mathbf{z}})) \quad (2)$$

3.3. Semantics Composition Generation

Upon obtaining the reconstructed latent code \hat{z}_c , we employ it as a condition, which is integrated into the diffusion model’s U-Net architecture [26] via a control module \mathcal{C} [64]. The control module has the same architecture as the diffusion U-Net encoder and uses several zero-convolutional layers to inject conditional knowledge into the diffusion process. The diffusion model, trained extensively on a vast dataset of images, effectively captures the distribution of images. Therefore, even with merely coarse information about the background, the diffusion model can utilize its prior knowledge to adequately inpaint this aspect, and compose the task-related objects effectively to construct a high-quality, complete image, thereby satisfying human perception criteria.

Specifically, given an initial noise z_T and the condition \hat{z}_c , we employ the reverse process of the diffusion model to iteratively denoise as follows:

$$z_{t-1} = \frac{1}{\sqrt{\alpha_t}} \left(z_t - \frac{\sqrt{1-\alpha_t}}{\sqrt{1-\alpha_t}} \epsilon_\theta(z_t, t, \mathcal{C}(\hat{z}_c)) \right) \quad (3)$$

Here, $\epsilon_\theta(\cdot)$ represents the U-Net within the diffusion model, tasked to predict the noise at each step, with parameters denoted by θ . α_t represents a scaling factor that determines how much noise is added to the latent variable z_t at step t . After iterating T cycles, we obtain the denoised latent representation z_0 , which is then inputted into the diffusion VAE decoder \mathcal{D} to produce the final reconstructed image $\hat{\mathbf{x}}$.

In Figure 4, we present several visualization results to demonstrate the feasibility of compositional generation through the task-related regions along with side priors. We attempt to reconstruct z_c , which is obtained by inputting the original image into the VAE diffusion encoder \mathcal{E} , as accurately as possible using the partial task-related compressed latent $\tilde{\mathbf{y}}_i$. Using the information from this $\tilde{\mathbf{y}}_i$ along with coarse global information from side priors $\hat{\mathbf{z}}$, we can obtain a rough reconstruction of z_c . Subsequently, leveraging the diffusion prior, we refine z_c to obtain a denoised latent z_0 , which is then passed through the diffusion VAE decoder to yield the reconstructed full high-quality image $\hat{\mathbf{x}}$. It can be observed that the z_0 generated by diffusion is very similar to the ground truth z_c in Fig. 4, thereby facilitating the production of a high-quality reconstructed image $\hat{\mathbf{x}}$.

3.4. Training Strategy

To implement the aforementioned pipeline for analysis, disentanglement, and composition, we divide our training

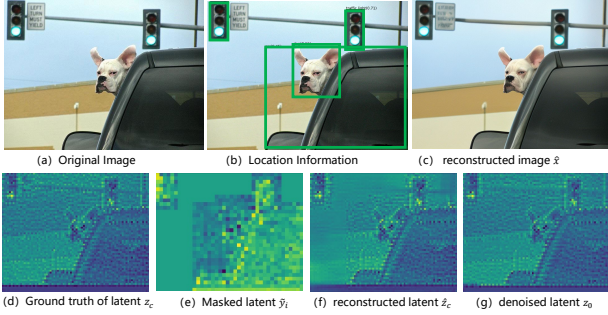


Figure 4. Visualization of the intermediate process in semantics composition generation. DISCOVER can use the partial task-related compressed latent \tilde{y}_i to generate high quality image \hat{x} .

steps into two stages. In the first stage, semantic analysis and disentanglement are not introduced, instead, we train a diffusion-based codec end-to-end. The specific loss function is defined as follows:

$$\mathcal{L}_I = \lambda_R(R(\hat{y}) + R(\hat{z})) + \lambda_{diff} \|\epsilon - \epsilon_\theta(z_t, t, \mathcal{C}(\hat{z}_c))\|^2 + \|z_c - \hat{z}_c\|^2, \quad (4)$$

where $R(\hat{y})$ and $R(\hat{z})$ are the rate loss, used to constrain the bitrate of the compressed bitstream. The second term measures the discrepancy between the U-Net’s predicted noise and the actual noise ϵ , while the third term captures the difference between the latent code \hat{z}_c output at the decoder side and the latent code z_c obtained from the original image through the diffusion encoder \mathcal{E} , facilitating training stability and accelerating convergence. During this training phase, the diffusion weights, sourced from the pretrained Stable Diffusion 2.1 [26], remain frozen, and only the parameters of the control module and codec are updated.

In the second stage of training, we attempt to endow the codec with the capabilities for disentanglement and generation. Specifically, we apply random masks to the latent code \hat{y} during training, ensuring that only partial information along with coarse global side information is transmitted to the decoder, allowing the model to generate based on this partial information. To maintain training stability in this phase, the parameters of the encoder and the hyper-prior path within the codec remain frozen, and only the decoder is updated. The diffusion component still undergoes updates solely in the control module. The difference in the loss function from the first stage lies in the replacement of $R(\hat{y})$ with rate loss for partial region parts $R(\hat{y})$.

4. Experiments

4.1. Experimental Settings

4.1.1 Implementation Details

We utilize ChatGPT-4o [24] and GroundingDINO 1.0 [25] (Swin-Tiny backbone) as the models for semantic analysis,

keeping them frozen throughout the process without involving them in training stages. ELIC [65] serves as our base codec. The last two layers of its decoder are removed to align with the size of the diffusion latent code. In both training stages I and II, λ_{diff} is set to 2, while λ_R is chosen from $\{1, 2, 4, 8\}$ in Equation 4 to achieve models with varying bitrates. For the diffusion model, we employ Stable Diffusion 2.1-base [26] as the generative model, and the sampling step is set as 8 for machine vision tasks, 50 for human perception tasks. More details about the sampling step can be found in supplementary materials. In Stage II, to enable the codec with disentangled and compositional generation capabilities, we randomly set 0~50% of the region in \hat{y} to zero during each forward pass before transmission to decoder. The training dataset comprises 50K images from OpenImage [66], alongside almost 10K high-resolution images from COCO train2017 [67], CLIC2020 training set [68], Flickr2K [69], and Div2K [70]. During the training, these images are randomly cropped to a size of 512x512. In the first stage, the model is trained for 300,000 iterations, followed by an additional 50,000 iterations in the Stage II.

Machine Vision. For machine vision tasks, we conduct evaluations on object detection, instance segmentation, and classification tasks. For detection and segmentation tasks, we use the MS COCO2017 val dataset with Faster R-CNN [13] and Mask RCNN [71] (R50-FPN) as downstream task networks. For the classification task, we test ResNet-50 [72] on ImageNet [73].

Human Perception. For human perception, we performed evaluations on the Kodak [74], CLIC2020 [68], and COCO2017 val dataset. Following the setting in [75], for CLIC2020, images are resized so that the shorter edge is 768 pixels, followed by a center crop of 768x768 for evaluation.

4.1.2 Evaluation Protocol

Compression Ratio. In this work, bits per pixel (bpp) is used to measure the compression ratio. Following [19], bpp is formulated as: $\frac{b}{p}$, where b denotes the total bits cost of the all encoded bit-streams in the datasets. p represents the total pixels of the images in the dataset.

Machine Vision. In terms of evaluation metrics, for machine vision, we used Average Precision (AP) to evaluate performance in object detection and instance segmentation tasks, and accuracy for classification tasks.

Human Perception. For human perception, we used FID [76], KID [77], DISTS [78], and LPIPS [79] as evaluation metrics. Similar to [36], the images from CLIC are divided into 256x256 patches to compute FID and KID.

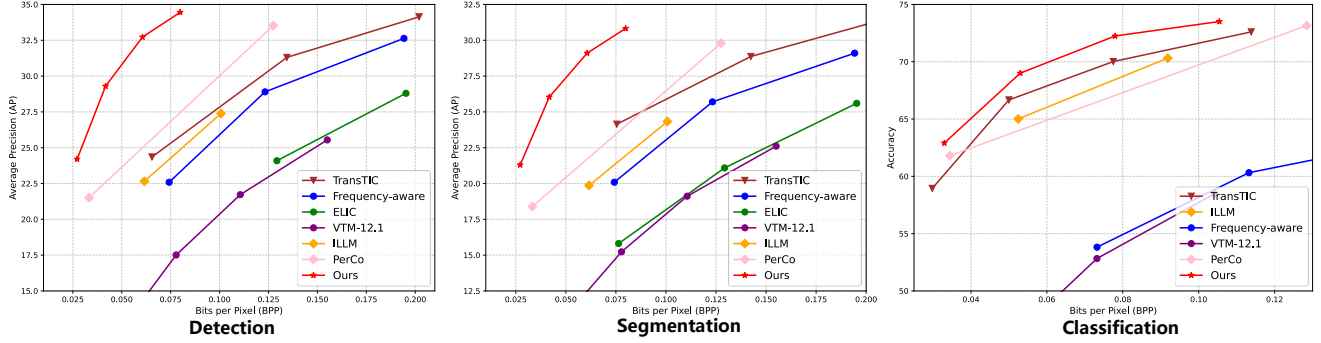


Figure 5. Machine vision tasks performance comparison. We use \diamond , ∇ , \circ to represent generative, image coding for machine, fidelity-based methods, respectively. Our method is represented by \star , and the proposed versatile method outperforms recent methods across three machine vision tasks without retraining while maintaining satisfactory human perception, as shown in Fig. 6.

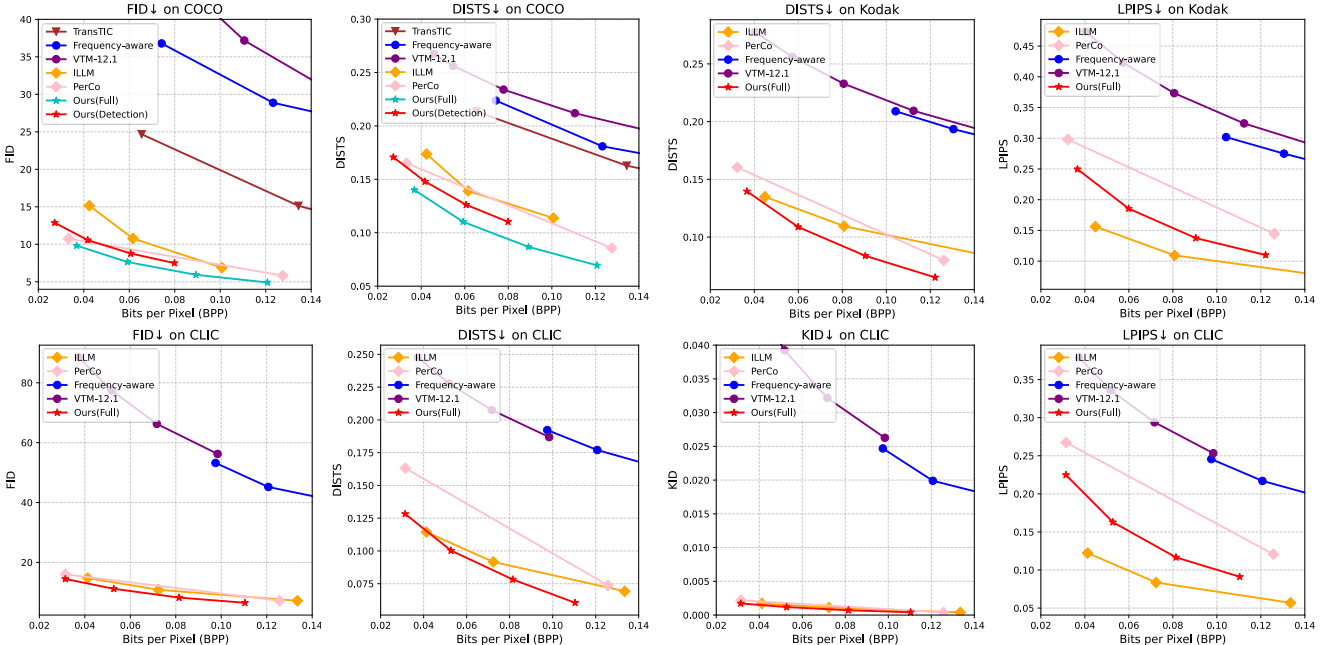


Figure 6. Human perception comparison. “Ours(Full)” means that all bitstreams are transmitted for reconstruction, while “Ours(Detection)” means that only disentangled task-related parts for detection task are transmitted.

4.1.3 Comparison Approaches

We conducted comparisons with three categories of methods: image coding for machine method (TransTIC [22]), which are designed for machine tasks, generative image compression methods (ILLM [9], PerCo [10]) tailored for human perception, and some fidelity-based approaches (Frequency-aware [5], ELIC [65] and VTM-12.1 [80]).

4.2. Performance Comparison

As illustrated in Fig. 5, we performed the comparison of machine vision tasks, including detection, segmentation, and classification. The SOTA diffusion-based method, PerCo [10], leverages the strong generative priors of diffusion models, achieving higher performance in detection tasks compared to image coding for machine method, TransTIC [22]. However, due to its general design rather

than a specific focus on machine vision, PerCo shows limitations in segmentation and classification. In contrast, our method employs semantic disentanglement to encode information according to the semantic requirements of each machine vision task. This targeted approach reduces the bits required for encoding information irrelevant to downstream tasks, resulting in improved performance across detection, segmentation, and classification tasks compared with other methods. Specifically, setting VTM-12.1 as the anchor, we can achieve BD-rates [30] of -80.41%, -80.32%, and -77.63% on these three tasks, respectively.

4.2.1 Human Perception

While achieving strong performance in machine vision tasks, our method also maintains high-quality human perception. As shown in the two subplots in the upper-left corner of Fig. 6, our method, after disentanglement for

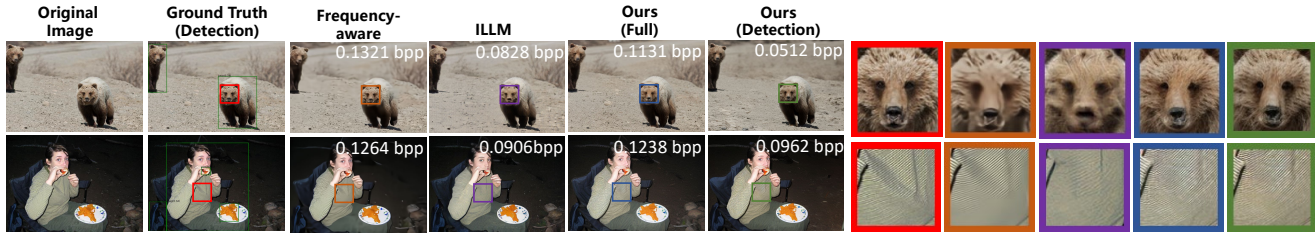


Figure 7. The visualization results. DISCOVER preserves information in task-related regions for machine vision tasks while effectively meeting human visual perception requirements. The scheme of “Ours (Detection)” means the reconstructed image of our method by transmitting only the partial task-related bit-stream, while “Ours (Full)” means the full bit-stream is transmitted. “Ground Truth (Detection)” means the results of grounding model, which indicates the task-related regions for the object detection task.

the detection task, can still reconstruct high-quality images (low FID and DISTS, i.e., -45.615 BD-FID and -0.123 BD-DISTS [31] by setting VTM-12.1 as the anchor) on the decoding side, outperforming both the generative method PerCo [10] and ILLM [9].

Moreover, by transmitting the full bit-stream, we can further enhance human perception quality. As demonstrated in Fig. 6, our method achieves superior human perception performance on the Kodak and CLIC datasets, outperforming other methods in FID, DISTS, and KID. Although the LPIPS of our method is slightly higher than that of ILLM due to the stochastic characteristic of diffusion, it remains superior to the counterpart diffusion-based method PerCo.

4.3. Ablation Study

In Fig. 8, we analyze the gains achieved through semantic disentanglement and generative enhancement. It can be observed that directly applying disentanglement without generative composition provides some performance improvements over the base codec. However, as the base codec is optimized for MSE rather than designed specifically for machine vision, and conducting disentanglement alone results in the loss of some contextual information, these factors together lead to performance bottlenecks in machine vision tasks. On the other hand, using generative composition alone yields substantial gains, yet since it is optimized for human eyes, and retains a considerable amount of redundant information for machine tasks. Our method leverages both disentanglement and composition processes, achieving further improvements in machine vision task performance, and also saving the bit costs.

4.4. Visualization

In Fig. 7, we present some visualized results. The figure shows that the fidelity-based method, Frequency-aware [5], results in blurring, particularly in complex textures, such as the striped clothing in the second row, it struggles to reconstruct details accurately. In contrast, our approach leverages the priors from diffusion, enabling more detailed reconstruction compared with the generative method ILLM [9]. For example, the bear’s face in the first row shows signif-

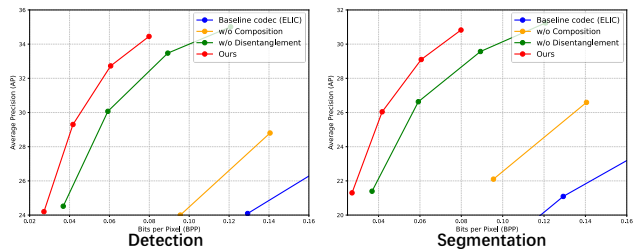


Figure 8. Ablation studies on COCO dataset. “w/o composition” means that on the decoder side, the generative model is not used and the reconstructed image is directly output through g_s . “w/o disentanglement” indicates that the latent code is not disentangled according to the task, and the full bit-stream is transmitted.

icant distortion in both ILLM and fidelity-based methods, while our method preserves more details.

Furthermore, we compared the reconstruction quality of transmitting only the task-related region bit-streams, Ours (Detection), versus the full bit-streams, Ours (Full). For task-related regions, both approaches achieve similar results indicating task-related information is well preserved. Additionally, by transmitting only the task-related region bit-stream, our method, with the help of diffusion priors, can effectively reconstruct approximate background information, satisfying human perception, while reducing a substantial bit cost.

5. Conclusion

In this paper, we introduce a new paradigm dubbed DISCOVER to image compression, addressing the different requirements of high-quality human visual perception and optimized performance for different machine vision tasks. We use multimodal large language models and grounding models to analyze the semantics of tasks and images, assisting with semantic disentanglement encoding. By leveraging semantic disentanglement, DISCOVER enables partially encoding that selectively transmits task-related information, significantly reducing bits cost. The following semantic composition decoding approach utilizes the diffusion model further enhances reconstruction, composing essential object details with prior side knowledge to generate high qual-

ity image and achieve both satisfactory human perception and diverse machine vision task performance. Experimental results underscore the robustness and versatility of our approach, demonstrating superior performance in both machine vision and human perception evaluations.

References

- [1] G. K. Wallace, “The jpeg still picture compression standard,” *IEEE transactions on consumer electronics*, vol. 38, no. 1, pp. xviii–xxxiv, 1992. 1, 2
- [2] G. J. Sullivan, J.-R. Ohm, W.-J. Han, and T. Wiegand, “Overview of the high efficiency video coding (hevc) standard,” *TCSVT*, vol. 22, no. 12, pp. 1649–1668, 2012. 1
- [3] B. Bross, Y.-K. Wang, Y. Ye, S. Liu, J. Chen, G. J. Sullivan, and J.-R. Ohm, “Overview of the versatile video coding (vvc) standard and its applications,” *TCSVT*, 2021. 1, 2
- [4] J. Liu, H. Sun, and J. Katto, “Learned image compression with mixed transformer-cnn architectures,” in *Proceedings of the IEEE/CVF Conference on Computer Vision and Pattern Recognition (CVPR)*, June 2023, pp. 14 388–14 397. 1, 2, 3, 5
- [5] H. Li, S. Li, W. Dai, C. Li, J. Zou, and H. Xiong, “Frequency-aware transformer for learned image compression,” *International Conference on Learning Representations*, 2024. 1, 3, 7, 8
- [6] Z. Cheng, H. Sun, M. Takeuchi, and J. Katto, “Learned image compression with discretized gaussian mixture likelihoods and attention modules,” in *CVPR*, 2020, pp. 7939–7948. 1, 2
- [7] C. Li, G. Lu, D. Feng, H. Wu, Z. Zhang, X. Liu, G. Zhai, W. Lin, and W. Zhang, “misc: Ultra-low bitrate image semantic compression driven by large multimodal model,” *arXiv preprint arXiv:2402.16749*, 2024. 1, 3
- [8] E. Agustsson, D. Minnen, G. Toderici, and F. Mentzer, “Multi-realism image compression with a conditional generator,” in *Proceedings of the IEEE/CVF Conference on Computer Vision and Pattern Recognition*, 2023, pp. 22 324–22 333. 3
- [9] M. J. Muckley, A. El-Nouby, K. Ullrich, H. Jégou, and J. Verbeek, “Improving statistical fidelity for neural image compression with implicit local likelihood models,” in *International Conference on Machine Learning*. PMLR, 2023, pp. 25 426–25 443. 7, 8
- [10] M. Careil, M. J. Muckley, J. Verbeek, and S. Lathuilière, “Towards image compression with perfect realism at ultra-low bitrates,” in *The Twelfth International Conference on Learning Representations*, 2024. 1, 3, 7, 8
- [11] J. Ballé, V. Laparra, and E. P. Simoncelli, “End-to-end optimized image compression,” in *ICLR*, 2017. 1, 2, 3
- [12] J. Ballé, D. Minnen, S. Singh, S. J. Hwang, and N. Johnston, “Variational image compression with a scale hyperprior,” in *ICLR*, 2018. 1, 3, 5
- [13] S. Ren, K. He, R. Girshick, and J. Sun, “Faster r-cnn: Towards real-time object detection with region proposal networks,” *NeurIPS*, vol. 28, pp. 91–99, 2015. 1, 6
- [14] A. Kirillov, E. Mintun, N. Ravi, H. Mao, C. Rolland, L. Gustafson, T. Xiao, S. Whitehead, A. C. Berg, W.-Y. Lo *et al.*, “Segment anything,” *arXiv preprint arXiv:2304.02643*, 2023.
- [15] A. Radford, J. W. Kim, C. Hallacy, A. Ramesh, G. Goh, S. Agarwal, G. Sastry, A. Askell, P. Mishkin, J. Clark *et al.*, “Learning transferable visual models from natural language supervision,” in *ICML*. PMLR, 2021, pp. 8748–8763. 1
- [16] B. Li, R. Wang, G. Wang, Y. Ge, Y. Ge, and Y. Shan, “Seed-bench: Benchmarking multimodal llms with generative comprehension,” *arXiv preprint arXiv:2307.16125*, 2023. 1
- [17] B. Li, J. Dong, Y. Wang, J. Liu, L. Yin, W. Zhao, Z. Zhu, X. Jin, and W. Zeng, “One at a time: Multi-step volumetric probability distribution diffusion for depth estimation,” *arXiv preprint arXiv:2306.12681*, 2023. 1
- [18] R. Feng, X. Jin, Z. Guo, R. Feng, Y. Gao, T. He, Z. Zhang, S. Sun, and Z. Chen, “Image coding for machines with omnipotent feature learning,” in *ECCV*. Springer, 2022, pp. 510–528. 2, 3
- [19] J. Liu, R. Feng, Y. Qi, Q. Chen, Z. Chen, W. Zeng, and X. Jin, “Rate-distortion-cognition controllable versatile neural image compression,” in *European Conference on Computer Vision*. Springer, 2025, pp. 329–348. 3, 6
- [20] C.-H. Kao, C. Chien, Y.-J. Tseng, Y.-H. Chen, A. Gnutti, S.-Y. Lo, W.-H. Peng, and R. Leonardi, “Comneck: Bridging compressed image latents and multimodal llms via universal transform-neck,” *arXiv preprint arXiv:2407.19651*, 2024.
- [21] H. Li, S. Li, S. Ding, W. Dai, M. Cao, C. Li, J. Zou, and H. Xiong, “Image compression for machine and human vision with spatial-frequency adaptation,” *European Conference on Computer Vision*, 2024. 2
- [22] Y.-H. Chen, Y.-C. Weng, C.-H. Kao, C. Chien, W.-C. Chiu, and W.-H. Peng, “Transtic: Transferring transformer-based image compression from human perception to machine perception,” in *Proceedings of the IEEE/CVF International Conference on Computer Vision*, 2023, pp. 23 297–23 307. 2, 3, 7
- [23] L. D. Chamain, F. Racapé, J. Bégaint, A. Pushparaja, and S. Feltman, “End-to-end optimized image compression for machines, a study,” in *2021 Data Com-*

- pression Conference (DCC)*. IEEE, 2021, pp. 163–172. 2
- [24] ChatGPT, “Gpt-4o version,” <https://chat.openai.com/chat>, 2024, accessed: June 14, 2024. 2, 3, 6
- [25] S. Liu, Z. Zeng, T. Ren, F. Li, H. Zhang, J. Yang, C. Li, J. Yang, H. Su, J. Zhu *et al.*, “Grounding dino: Marrying dino with grounded pre-training for open-set object detection,” *European Conference on Computer Vision*, 2024. 2, 3, 4, 5, 6
- [26] R. Rombach, A. Blattmann, D. Lorenz, P. Esser, and B. Ommer, “High-resolution image synthesis with latent diffusion models,” in *in Proceedings of the IEEE/CVF Conference on Computer Vision and Pattern Recognition*, 2022. 2, 3, 5, 6
- [27] Z. Zheng, X. Peng, T. Yang, C. Shen, S. Li, H. Liu, Y. Zhou, T. Li, and Y. You, “Open-sora: Democratizing efficient video production for all,” March 2024. [Online]. Available: <https://github.com/hpcaitech/Open-Sora> 2
- [28] Y. Liu, K. Zhang, Y. Li, Z. Yan, C. Gao, R. Chen, Z. Yuan, Y. Huang, H. Sun, J. Gao *et al.*, “Sora: A review on background, technology, limitations, and opportunities of large vision models,” *arXiv preprint arXiv:2402.17177*, 2024.
- [29] C. Saharia, W. Chan, S. Saxena, L. Li, J. Whang, E. L. Denton, K. Ghasemipour, R. Gontijo Lopes, B. Karagol Ayan, T. Salimans *et al.*, “Photorealistic text-to-image diffusion models with deep language understanding,” *Advances in neural information processing systems*, vol. 35, pp. 36479–36494, 2022. 2
- [30] G. Bjøntegaard, “Calculation of average psnr differences between rd-curves,” 2001. [Online]. Available: <https://api.semanticscholar.org/CorpusID:61598325> 2, 7
- [31] T. Xu, Q. Zhang, Y. Li, D. He, Z. Wang, Y. Wang, H. Qin, Y. Wang, J. Liu, and Y.-Q. Zhang, “Conditional perceptual quality preserving image compression,” *arXiv preprint arXiv:2308.08154*, 2023. 2, 8
- [32] M. Rabbani and R. Joshi, “An overview of the jpeg 2000 still image compression standard,” *Signal processing: Image communication*, vol. 17, no. 1, pp. 3–48, 2002. 2
- [33] T. Wiegand, G. J. Sullivan, G. Bjontegaard, and A. Luthra, “Overview of the h. 264/avc video coding standard,” *TCSVT*, vol. 13, no. 7, pp. 560–576, 2003. 2
- [34] D. Minnen, J. Ballé, and G. Toderici, “Joint autoregressive and hierarchical priors for learned image compression,” in *NeurIPS*, 2018. 2
- [35] F. Mentzer, E. Agustsson, M. Tschannen, R. Timofte, and L. Van Gool, “Conditional probability models for deep image compression,” in *CVPR*, 2018, pp. 4394–4402.
- [36] F. Mentzer, G. Toderici, M. Tschannen, and E. Agustsson, “High-fidelity generative image compression,” *Advances in neural information processing systems*, 2020. 2, 3, 6
- [37] R. Zhang, R. Fang, P. Gao, W. Zhang, K. Li, J. Dai, Y. Qiao, and H. Li, “Tip-adapter: Training-free clip-adapter for better vision-language modeling,” *arXiv preprint arXiv:2111.03930*, 2021. 2
- [38] T. He, S. Sun, Z. Guo, and Z. Chen, “Beyond coding: Detection-driven image compression with semantically structured bit-stream,” in *2019 Picture Coding Symposium (PCS)*. IEEE, 2019, pp. 1–5. 2
- [39] L. Duan, J. Liu, W. Yang, T. Huang, and W. Gao, “Video coding for machines: A paradigm of collaborative compression and intelligent analytics,” *TIP*, vol. 29, pp. 8680–8695, 2020.
- [40] S. Sun, T. He, and Z. Chen, “Semantic structured image coding framework for multiple intelligent applications,” *TCSVT*, 2020.
- [41] X. Jin, R. Feng, S. Sun, R. Feng, T. He, and Z. Chen, “Semantical video coding: Instill static-dynamic clues into structured bitstream for ai tasks,” *Journal of Visual Communication and Image Representation*, vol. 93, p. 103816, 2023.
- [42] J. Liu, H. Sun, and J. Katto, “Semantic segmentation in learned compressed domain,” in *2022 Picture Coding Symposium (PCS)*. IEEE, 2022, pp. 181–185.
- [43] J. Liu, X. Jin, R. Feng, Z. Chen, and W. Zeng, “Composable coding for machine via task-oriented internal adaptor and external prior,” in *2023 IEEE International Conference on Visual Communications and Image Processing (VCIP)*. IEEE, 2023, pp. 1–5. 2
- [44] Z. Yang, L. Li, K. Lin, J. Wang, C.-C. Lin, Z. Liu, and L. Wang, “The dawn of Imms: Preliminary explorations with gpt-4v(ision),” *arXiv preprint arXiv:2309.17421*, vol. 9, no. 1, p. 1, 2023. 3
- [45] H. Liu, C. Li, Q. Wu, and Y. J. Lee, “Visual instruction tuning,” *Advances in neural information processing systems*, vol. 36, 2024. 3
- [46] H. You, H. Zhang, Z. Gan, X. Du, B. Zhang, Z. Wang, L. Cao, S.-F. Chang, and Y. Yang, “Ferret: Refer and ground anything anywhere at any granularity,” *arXiv preprint arXiv:2310.07704*, 2023. 3
- [47] D. Zhu, J. Chen, X. Shen, X. Li, and M. Elhoseiny, “Minigt-4: Enhancing vision-language understanding with advanced large language models,” *arXiv preprint arXiv:2304.10592*, 2023. 3
- [48] G. Team, P. Georgiev, V. I. Lei, R. Burnell, L. Bai, A. Gulati, G. Tanzer, D. Vincent, Z. Pan, S. Wang *et al.*, “Gemini 1.5: Unlocking multimodal understanding across millions of tokens of context,” *arXiv preprint arXiv:2403.05530*, 2024.

- [49] R. Anil, S. Borgeaud, Y. Wu, J.-B. Alayrac, J. Yu, R. Soricut, J. Schalkwyk, A. M. Dai, A. Hauth, K. Millican *et al.*, “Gemini: A family of highly capable multimodal models,” *arXiv preprint arXiv:2312.11805*, vol. 1, 2023. 3
- [50] L. Yao, L. Li, S. Ren, L. Wang, Y. Liu, X. Sun, and L. Hou, “Deco: Decoupling token compression from semantic abstraction in multimodal large language models,” *arXiv preprint arXiv:2405.20985*, 2024. 3
- [51] B. McKinzie, Z. Gan, J.-P. Fauconnier, S. Dodge, B. Zhang, P. Dufter, D. Shah, X. Du, F. Peng, F. Weers *et al.*, “Mm1: Methods, analysis & insights from multimodal llm pre-training,” *arXiv preprint arXiv:2403.09611*, 2024. 3
- [52] Z. Yang, B. Gong, L. Wang, W. Huang, D. Yu, and J. Luo, “A fast and accurate one-stage approach to visual grounding,” in *Proceedings of the IEEE/CVF international conference on computer vision*, 2019, pp. 4683–4693. 3
- [53] Y. Liao, S. Liu, G. Li, F. Wang, Y. Chen, C. Qian, and B. Li, “A real-time cross-modality correlation filtering method for referring expression comprehension,” in *Proceedings of the IEEE/CVF Conference on Computer Vision and Pattern Recognition*, 2020, pp. 10 880–10 889.
- [54] Z. Yang, T. Chen, L. Wang, and J. Luo, “Improving one-stage visual grounding by recursive sub-query construction,” in *Computer Vision—ECCV 2020: 16th European Conference, Glasgow, UK, August 23–28, 2020, Proceedings, Part XIV 16*. Springer, 2020, pp. 387–404. 3
- [55] O. Avrahami, D. Lischinski, and O. Fried, “Blended diffusion for text-driven editing of natural images,” in *Proceedings of the IEEE/CVF conference on computer vision and pattern recognition*, 2022, pp. 18 208–18 218. 3
- [56] G. Couairon, J. Verbeek, H. Schwenk, and M. Cord, “Diffedit: Diffusion-based semantic image editing with mask guidance,” *arXiv preprint arXiv:2210.11427*, 2022.
- [57] C. Meng, Y. He, Y. Song, J. Song, J. Wu, J.-Y. Zhu, and S. Ermon, “Sdedit: Guided image synthesis and editing with stochastic differential equations,” *arXiv preprint arXiv:2108.01073*, 2021.
- [58] G. Parmar, K. Kumar Singh, R. Zhang, Y. Li, J. Lu, and J.-Y. Zhu, “Zero-shot image-to-image translation,” in *ACM SIGGRAPH 2023 Conference Proceedings*, 2023, pp. 1–11. 3
- [59] M. Akbari, J. Liang, and J. Han, “Dsslic: Deep semantic segmentation-based layered image compression,” in *ICASSP 2019-2019 IEEE International Conference on Acoustics, Speech and Signal Processing (ICASSP)*. IEEE, 2019, pp. 2042–2046. 3
- [60] J. Liu, H. Sun, and J. Katto, “Learning in compressed domain for faster machine vision tasks,” in *2021 International Conference on Visual Communications and Image Processing (VCIP)*. IEEE, 2021, pp. 01–05. 3
- [61] N. Körber, E. Kromer, A. Siebert, S. Hauke, D. Mueller-Gritschneider, and B. Schuller, “Egic: Enhanced low-bit-rate generative image compression guided by semantic segmentation,” in *European Conference on Computer Vision*. Springer, 2025, pp. 202–220. 3
- [62] J. D. M.-W. C. Kenton and L. K. Toutanova, “Bert: Pre-training of deep bidirectional transformers for language understanding,” in *Proceedings of naacL-HLT*, vol. 1. Minneapolis, Minnesota, 2019, p. 2. 4
- [63] Z. Liu, Y. Lin, Y. Cao, H. Hu, Y. Wei, Z. Zhang, S. Lin, and B. Guo, “Swin transformer: Hierarchical vision transformer using shifted windows,” in *Proceedings of the IEEE/CVF international conference on computer vision*, 2021, pp. 10 012–10 022. 4
- [64] L. Zhang, A. Rao, and M. Agrawala, “Adding conditional control to text-to-image diffusion models,” in *Proceedings of the IEEE/CVF International Conference on Computer Vision*, 2023, pp. 3836–3847. 5
- [65] D. He, Z. Yang, W. Peng, R. Ma, H. Qin, and Y. Wang, “Elic: Efficient learned image compression with unevenly grouped space-channel contextual adaptive coding,” in *Proceedings of the IEEE/CVF Conference on Computer Vision and Pattern Recognition*, 2022, pp. 5718–5727. 6, 7
- [66] A. Kuznetsova, H. Rom, N. Alldrin, J. Uijlings, I. Krasin, J. Pont-Tuset, S. Kamali, S. Popov, M. Mallocci, A. Kolesnikov, T. Duerig, and V. Ferrari, “The open images dataset v4: Unified image classification, object detection, and visual relationship detection at scale,” *IJCV*, 2020. 6
- [67] T.-Y. Lin, M. Maire, S. Belongie, J. Hays, P. Perona, D. Ramanan, P. Dollár, and C. L. Zitnick, “Microsoft coco: Common objects in context,” in *ECCV*. Springer, 2014, pp. 740–755. 6
- [68] CLIC, “Workshop and challenge on learned image compression,” in *Proceedings of the IEEE/CVF Conference on Computer Vision and Pattern Recognition*, 2021. 6
- [69] B. Lim, S. Son, H. Kim, S. Nah, and K. M. Lee, “Enhanced deep residual networks for single image super-resolution,” in *The IEEE Conference on Computer Vision and Pattern Recognition (CVPR) Workshops*, July 2017. 6
- [70] E. Agustsson and R. Timofte, “Ntire 2017 challenge on single image super-resolution: Dataset and study,” in *The IEEE Conference on Computer Vision and Pattern Recognition (CVPR) Workshops*, July 2017. 6

- [71] K. He, G. Gkioxari, P. Dollár, and R. Girshick, “Mask r-cnn,” in *ICCV*, 2017, pp. 2961–2969. [6](#)
- [72] K. He, X. Zhang, S. Ren, and J. Sun, “Deep residual learning for image recognition,” in *CVPR*, 2016, pp. 770–778. [6](#)
- [73] J. Deng, “A large-scale hierarchical image database,” *Proceedings of IEEE/CVF conference on Computer Vision and Pattern Recognition*, 2009. [6](#)
- [74] E. Kodak, “Kodak lossless true color image suite (photo cd pcd0992),” 1993. [6](#)
- [75] R. Yang and S. Mandt, “Lossy image compression with conditional diffusion models,” *Advances in Neural Information Processing Systems*, vol. 36, 2024. [6](#)
- [76] M. Heusel, H. Ramsauer, T. Unterthiner, B. Nessler, and S. Hochreiter, “Gans trained by a two time-scale update rule converge to a local nash equilibrium,” *Advances in neural information processing systems*, vol. 30, 2017. [6](#)
- [77] M. Bińkowski, D. J. Sutherland, M. Arbel, and A. Gretton, “Demystifying mmd gans,” *arXiv preprint arXiv:1801.01401*, 2018. [6](#)
- [78] K. Ding, K. Ma, S. Wang, and E. P. Simoncelli, “Image quality assessment: Unifying structure and texture similarity,” *IEEE transactions on pattern analysis and machine intelligence*, vol. 44, no. 5, pp. 2567–2581, 2020. [6](#)
- [79] R. Zhang, P. Isola, A. A. Efros, E. Shechtman, and O. Wang, “The unreasonable effectiveness of deep features as a perceptual metric,” in *Proceedings of the IEEE conference on computer vision and pattern recognition*, 2018, pp. 586–595. [6](#)
- [80] J. V. E. Team, “Vvc official test model vtm.” 2021. [7](#)